Matthias Braun*
Job Duarte da Costa
Renata Obiala
Christoph Odenbreit

DOI: 10.1002/stco.201610007

Design of single-span beams for SLS and ULS using semi-continuous beam-to-column joints

Part 1: Beams with constant bending stiffness and joints according to EN 1993-1-8

This article explains a method for determining how semi-continuous joints influence the deflection, natural frequency and bending moment distribution of single-span beams with constant inertia under uniformly distributed load. The method is adequate for simple hand calculations, allowing the structural engineer to assess potential savings already in the pre-design phase. Further, the economical potential of semi-continuous joints according to EN 1993-1-8 [1] is demonstrated by an application example.

1 Introduction

Modern construction demands long-span structures that allow huge spaces free from columns, easily convertible for future use. Further, the structures have to be economic, which requires low material consumption and simple erection processes, and they have to be sustainable. To satisfy such demand for economic structures with long beam spans, floor beams need a high loadbearing resistance and stiffness. The utilization of high-strength steel grades fulfils the requirement of a high loadbearing resistance, but it does not improve the bending stiffness. It is the activation of a composite action between steel beam and concrete slab that increases the beam stiffness significantly [2], [3]; further optimization of the floor beam cross-section can be achieved by using semi-continuous beam-to-column joints. Semi-continuous joints influence the distribution of the bending moment along the beam, leading to the desired decrease in the beam deflection and increase in the natural frequency of the beam in comparison with simple, hinged beam-to-column joints.

Design rules for semi-continuous beam-to-column joints in steel are given in [1]. Standard design software allows the moment–rotation characteristic of the joint to be quickly determined. But to assess the influence of those joints on the beam behaviour at ULS and SLS, the moment–rotation characteristic has to be implemented in the global analyses, which requires additional effort by the structural engineer.

This article gives formulae that allow easy determination of the influence of semi-continuous joints on the beam deflection, natural frequency and distribution of the internal forces in a single-span floor beam with constant bending stiffness and subjected to a uniformly distributed load. The formulae derived can help engineers, practitioners and students to reach a better understanding of the influence of semi-continuous joints on the beam behaviour at ULS and SLS. The analytical equations given were used to determine factors, thus allowing quick, easy and safe application. Further contributions are planned, covering the use of semi-continuous joints for beams with partially constant stiffness (composite beams) and composite beam-to-column joints.

2 Global analysis

In a global analysis, the effects of the behaviour of the joints on the distribution of internal forces within a structure, and on the overall deformations of the structure, should generally be taken into account. However, as these effects are sufficiently small for nominally pinned and rigid/full-strength joints, they may therefore be neglected. Three basic methods of global analysis exist:

Elastic global analysis
The distribution of the internal forces within the structure only depends on the stiffness of the members in the structure. Therefore, joints should be classified according to their stiffness. In the case of a semi-rigid joint, the rotational stiffness S_j corresponding to the bending moment $M_{j,Ed}$ should generally be used in the analysis. As a simplification, the rotational stiffness may be taken as $S_{j,ini}/\eta$ in the analysis for all values of the moment $M_{j,Ed} \leq M_{j,Rd}$, where a value of 2.0 for the stiffness modification coefficient η can be used for typical beam-to-column joints. For other types of joint, see Table 5.2 in [1]. If $M_{j,Ed}$ does not exceed 2/3 of $M_{j,Rd}$, the initial rotational stiffness $S_{j,ini}$ may be used in the global analysis.

Rigid–plastic global analysis
Using rigid–plastic global analysis, the distribution of the internal forces within the structure only depends on the strength of the members in the structure. Therefore, joints should be classified according to their strength. The rotational capacity of a joint should be sufficient to accommodate the rotations resulting from the analysis.

* Corresponding author:
mathias.braun@arcelormittal.com

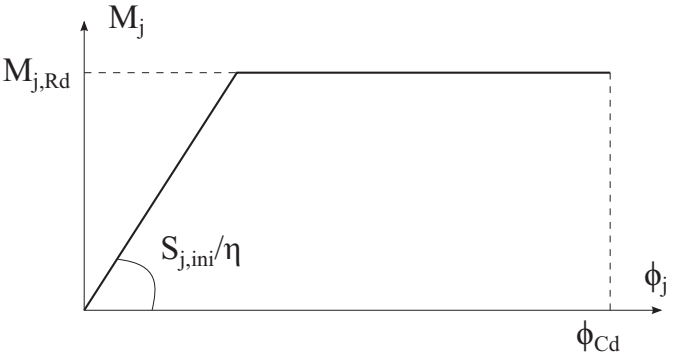

Fig. 1. Simplified bi-linear design moment–rotation characteristic for elastic–plastic global analysis

Elastic–plastic global analysis

The distribution of the internal forces within the structure depends on the stiffness and strength of the structural members. Therefore, joints should be classified according to both stiffness and strength. The moment–rotation characteristic of the joints should be used to determine the distribution of internal forces. As a simplification to the non-linear moment–rotation behaviour of a joint, a bi-linear design moment–rotation characteristic may be adopted, see Fig. 1. For the determination of the stiffness coefficient η, see Table 5.2 in [1].

The appropriate type of joint model should be determined from Table 1, depending on the classification of the joint and on the chosen method of analysis. The design moment–rotation characteristic of a joint used in the analysis may be simplified by adopting any appropriate curve, including a linearized approximation (e.g. bi- or tri-linear), provided that the approximate curve lies entirely below the design moment–rotation characteristic.

3 Economical structures with semi-continuous joints

As shown in section 2, the type of beam-to-column joint has a significant influence on the distribution of the internal forces along the beam and, consequently, on the beam design. Whereas nominally pinned beam-to-column joints lead to a higher bending moment at mid-span, they are popular in buildings due to their low fabrication cost. A comparison of the bending moments for simple, hinged beam-to-column joints with fully rigid joints is given in Fig. 2. The rotational stiffness of the semi-continuous joint is represented at its adjacent support A and B by a rotational spring $S_{j,A}$ and $S_{j,B}$ respectively. As shown, fully rigid joints reduce the bending moment at mid-span by a factor of three by creating a bending moment at the supports. Hence, they lead to a more economic distribution of the internal forces along the beam span, enabling the use of a smaller beam section and thus reducing material consumption and costs. On the other hand, however, the fabrication costs for fully rigid joints are much higher than that for pinned joints. The economic optimum between fabrication and material costs is achieved by using semi-continuous joints, see Fig. 3. Semi-continuous joints allow for the transmission of a bending moment via the joint and for a certain rotation of the joint, which – compared with rigid joints – leads to a higher bending moment at mid-span, requiring a bigger beam section. But they are much more economic than rigid joints. An optimum (= minimum total cost) has to be calculated for each structure individually.

Table 1. Type of joint model for global analysis according to [1]

Method of global analysis	Classification of joint		
Elastic	Nominally pinned	Rigid	Semi-rigid
Rigid-Plastic	Nominally pinned	Full-strength	Partial-strength
Elastic-Plastic	Nominally pinned	Rigid and full-strength	Semi-rigid and partial-strength Semi-rigid and full-strength Rigid and partial-strength
Type of joint model	Simple	Continuous	Semi-continuous

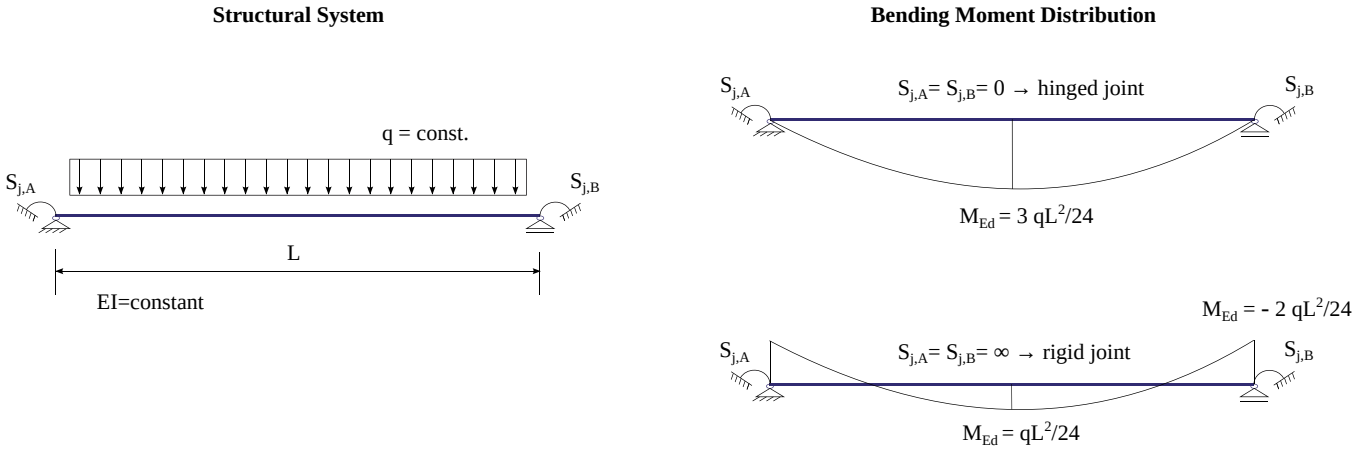

Fig. 2. Bending moment distribution for nominally pinned and rigid joints

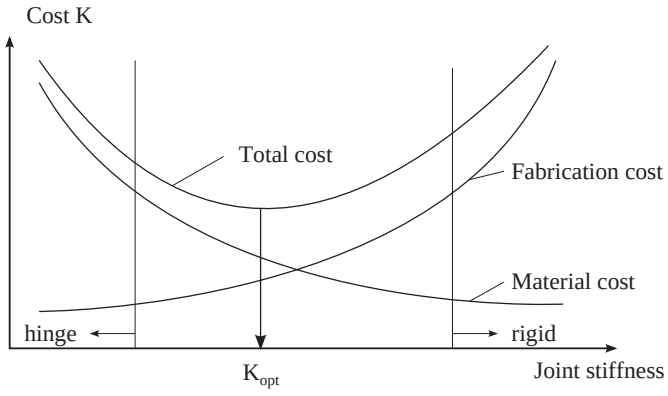

Fig. 3. Total cost as a function of the joint stiffness according to [4]

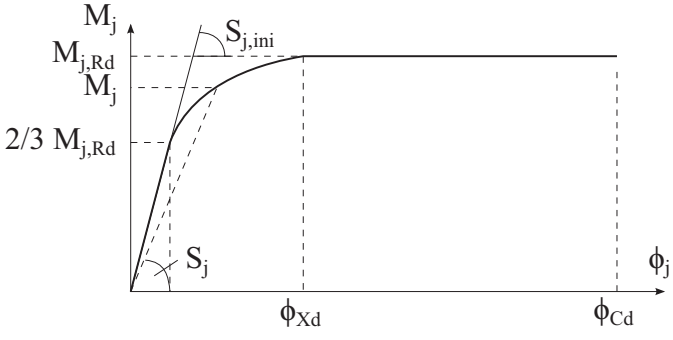

Fig. 4. Design moment–rotation characteristic for a joint

4 Joint design according to EN 1993-1-8

4.1 Design moment–rotation characteristic of a joint

A joint is classified using its design moment–rotation curve, which is characterized by its rotational stiffness S_j, its design moment resistance $M_{j,Rd}$ with corresponding rotation ϕ_{Xd} and its design rotational capacity ϕ_{Cd}, see Fig. 4.

- The rotational stiffness S_j is the secant stiffness as indicated in Fig. 4. The definition of S_j applies up to the rotation ϕ_{Xd} at which $M_{j,Ed}$ first reaches $M_{j,Rd}$. The initial stiffness $S_{j,ini}$ is the slope of the elastic range of the design moment–rotation characteristic.
- The design moment resistance $M_{j,Rd}$ is equal to the maximum moment of the design moment–rotation characteristic.
- The design rotation capacity ϕ_{Cd} is equal to the maximum rotation of the design moment–rotation characteristic.

Rules for calculating those values are given in [1].

4.2 Classification of joints

Joints may be classified by their rotational stiffness $S_{j,ini}$, their strength $M_{j,Rd}$ and their rotational capacity ϕ_{Cd}, see section 5.2 of [1] and Table 1.

Classification by stiffness

Classifying a joint by its rotational stiffness is performed by comparing its initial rotational stiffness $S_{j,ini}$ with the classification boundaries given in Fig. 5.

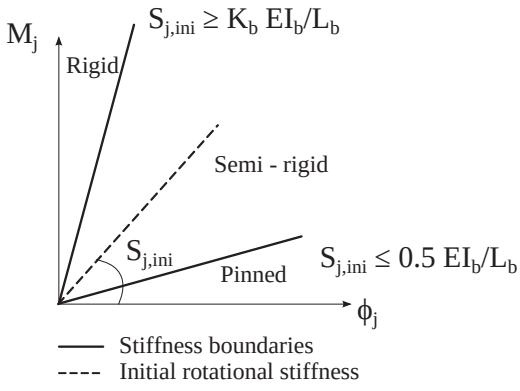

Fig. 5. Classification of beam-to-column joints by stiffness

where:

K_b = 8 for frames where the bracing system reduces the horizontal displacement by at least 80 %
E elastic modulus of beam material
I_b second moment of area of beam
L_b beam span (distance between centres of supporting columns)

Nominally pinned joints transmit the internal forces without developing significant moments and they should be capable of accepting the resulting rotations under the design loads. For rigid joints it is assumed that their rotational behaviour has no significant influence on the distribution of internal forces. Semi-rigid joints have a rotational stiffness that allows the transmission of a moment based on their design moment–rotation characteristic and their initial joint stiffness $S_{j,ini}$, see Fig. 5.

Classification by strength

According to its strength, a joint may be classified as full-strength, nominally pinned or partial-strength by comparing its design moment resistance $M_{j,Rd}$ with the design moment resistance of the members it connects, see Fig. 6. Nominally pinned joints transmit the internal forces without developing significant moments and should be capable of accepting the resulting rotations under the design loads. A joint may be classified as nominally pinned if its design moment resistance $M_{j,Rd}$ is not greater than 0.25 times the design moment resistance required for a full-strength joint, provided it also has sufficient rotational capacity. A joint may be classified as full-strength if it meets the criteria given in Fig. 6. A joint may be classified as a partial-strength joint if it does not meet the criteria for a full-strength or a nominally pinned joint.

Classification by rotational capacity

Using rigid–plastic global analysis and with the joint at a plastic hinge location, then for joints with a bending resistance $M_{j,Rd} < 1.2$ times the design plastic bending moment $M_{pl,Rd}$ of the cross-section of the connected member, the rotational capacity of the joint has to be checked. If the design resistance $M_{j,Rd}$ of a bolted joint is not governed by the design resistance of its bolts in shear or the design resistance of the welds and local instability does not occur, it may be assumed to have adequate rotational capacity for plastic global analysis. For more details, see 6.4 of [1] and

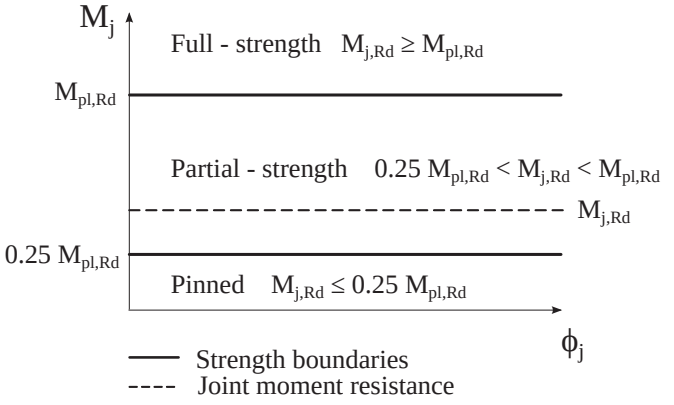

a) Top of column

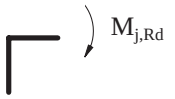

Either $M_{j,Rd} \geq M_{b,pl,Rd}$
or $M_{j,Rd} \geq M_{c,pl,Rd}$

b) within column height

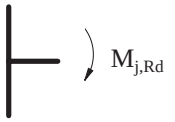

Either $M_{j,Rd} \geq M_{b,pl,Rd}$
or $M_{j,Rd} \geq 2\ M_{c,pl,Rd}$

$M_{b,pl,Rd}$ is the design plastic moment resistance of a beam
$M_{c,pl,Rd}$ is the design plastic moment resistance of a column

Fig. 6. Classification of joints by strength

[5]. The rules given in [1] are valid for steel grades S235, S275 and S355 and for joints for which the design value of the axial force N_{Ed} in the connected member does not exceed 5 % of the plastic design resistance $N_{pl,Rd}$ of its cross-section.

4.3 Simplified prediction of the initial joint stiffness

The rotational stiffness of a joint can be calculated with the rules given in section 6.3 of [1]. But to apply them, the joint first has to be defined, which requires knowledge about the distribution of the internal forces in the structure and especially at the positions of the joints. As the stiffness of the joint influences the distribution of the internal forces, the aforementioned process for determining the internal forces and the joint design is iterative. This process could be simplified if the designer could assess the initial joint stiffness adequately before the distribution of the internal forces is calculated, or at least when the basic dimensions of the sections are known.

A method described in [6] allows the initial stiffness of a joint to be assessed, which can be used in the preliminary design phase using simplified formulae. The designer can determine the stiffness of a joint just by selecting the basic joint configuration and taking account of some fixed choices regarding the connection detailing, e.g. for end-plate connections:

- The connection has only two bolt rows in tension.
- The bolt diameter is approx. 1.5 times the column flange thickness.
- The location of the bolt is as close as possible to the root radius of the column flange, the beam web and beam flange (about 1.5 times the thickness of the column flange).
- The end-plate thickness is similar to the column flange thickness.

For other joint types see [6]. The approximate value of the initial joint stiffness $S_{j,app}$ is expressed by

$$S_{j,app} = \frac{E \cdot z^2 \cdot t_{fc}}{C} \quad (1)$$

where the values of C for different joint configurations and loadings are given in Table 2, parameter z is the distance between the compression and tensile resultants and t_{fc} is the column flange thickness.

After calculating the distribution of the internal forces in the structure using $S_{j,app}$, it is necessary to check if this assumption was adequate. Fig. 7 shows the upper and lower boundaries for semi-continuous joints in braced frames. If the re-calculated value of $S_{j,ini}$ is within the given boundaries, the difference between stiffness $S_{j,app}$ and $S_{j,ini}$ affects the frame's loadbearing capacity by no more than 5 %. If $S_{j,ini}$ is not within the given boundaries, the calculation of the internal forces has to be repeated with an adapted joint stiffness.

5 Analytical investigations of the influence of semi-continuous joints on the behaviour of single-span beams

5.1 Assumptions

The equations for estimating the influence of semi-continuous beam-to-column joints on the overall beam behaviour

Table 2. Approximate determination of joint stiffness $S_{j,app}$ according to [6]

Joints with extended, unstiffened end-plate		Factor C
Single sided, ($\beta \approx 1$)	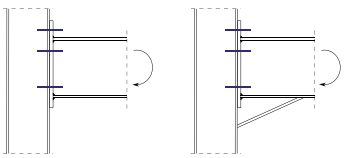	13
Double sided, ($\beta \approx 0$)	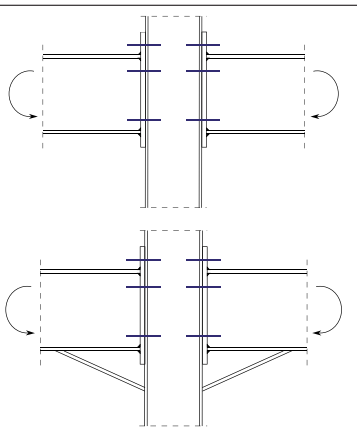	7.5

Note: For the rare cases of double-sided joint configurations where $\beta = 2$ (unbalanced moments), the value of the factor C is obtained by adding 11 to the relevant value for symmetrical conditions (balanced moments).

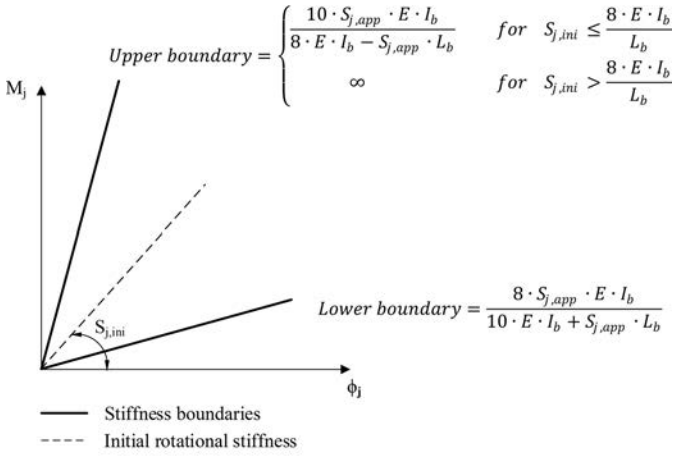

Fig. 7. Boundaries for discrepancy between $S_{j,app}$ and $S_{j,ini}$ for braced frames [6]

(ULS – distribution of inner forces, SLS – deflection and natural frequency) are derived in this section. Based on the equations obtained, factors are determined which simplify the use of semi-continuous joints, see Tables 3, 4 and 5. The rotational restraints at supports are represented by $S_{j,A}$ and $S_{j,B}$. The following assumptions were made, see Fig. 8:

- single-span beam
- constant bending stiffness EI
- uniformly distributed constant load and uniform mass distribution
- Euler-Bernoulli beam theory, shear deformations not considered
- first-order theory
- only vertical, harmonic vibration
- damping not considered
- linear moment–rotation (M_j-ϕ_j) relationship of rotational restraints

Table 3. Factors a and b for determining the maximum bending moment in the span and its position

k_B \ k_A	0.00	0.10	0.20	0.30	0.40	0.50	0.60	0.70	0.80	0.90	1.00
0.00 a = b =	1.50 0.50	Sym.	Sym.	Sym.	Sym.	Sym.	Sym.	Sym.	Sym.	Sym.	Sym.
0.10	1.45 0.51	1.40 0.50	Sym.	Sym.	Sym.	Sym.	Sym.	Sym.	Sym.	Sym.	Sym.
0.20	1.40 0.52	1.35 0.51	1.30 0.50	Sym.	Sym.	Sym.	Sym.	Sym.	Sym.	Sym.	Sym.
0.30	1.35 0.53	1.30 0.52	1.25 0.51	1.20 0.50	Sym.	Sym.	Sym.	Sym.	Sym.	Sym.	Sym.
0.40	1.31 0.53	1.25 0.53	1.20 0.52	1.15 0.51	1.10 0.50	Sym.	Sym.	Sym.	Sym.	Sym.	Sym.
0.50	1.26 0.54	1.21 0.53	1.15 0.52	1.10 0.52	1.05 0.51	1.00 0.50	Sym.	Sym.	Sym.	Sym.	Sym.
0.60	1.22 0.55	1.16 0.54	1.11 0.53	1.05 0.53	1.00 0.52	0.95 0.51	0.90 0.50	Sym.	Sym.	Sym.	Sym.
0.70	1.17 0.56	1.12 0.55	1.06 0.54	1.01 0.53	0.95 0.53	0.90 0.52	0.85 0.51	0.80 0.50	Sym.	Sym.	Sym.
0.80	1.13 0.57	1.07 0.56	1.02 0.55	0.96 0.54	0.91 0.53	0.85 0.53	0.80 0.52	0.75 0.51	0.70 0.50	Sym.	Sym.
0.90	1.08 0.58	1.03 0.57	0.97 0.56	0.92 0.55	0.86 0.54	0.81 0.53	0.75 0.53	0.70 0.52	0.65 0.51	0.60 0.50	Sym.
1.00	1.04 0.58	0.98 0.58	0.93 0.57	0.87 0.56	0.82 0.55	0.76 0.54	0.71 0.53	0.65 0.53	0.60 0.52	0.55 0.51	0.50 0.50
1.10	1.00 0.59	0.94 0.58	0.88 0.58	0.83 0.57	0.77 0.56	0.72 0.55	0.66 0.54	0.61 0.53	0.55 0.53	/	/
1.20	0.96 0.60	0.90 0.59	0.84 0.58	0.78 0.58	0.73 0.57	0.67 0.56	0.62 0.55	/	/	/	/
1.30	0.92 0.61	0.86 0.60	0.80 0.59	0.74 0.58	0.68 0.58	/	/	/	/	/	/
1.40	0.88 0.62	0.82 0.61	0.76 0.60	/	/	/	/	/	/	/	/
1.50	0.84 0.63	/	/	/	/	/	/	/	/	/	/

With $M_A = -\frac{q \cdot L^2}{12} \cdot k_A$; $M_B = -\frac{q \cdot L^2}{12} \cdot k_B$; max. $M_{Span} = \frac{q \cdot L^2}{12} \cdot a$ at $x_{max} = b \cdot L$

Table 4. Factors c and d for determining the maximum beam deflection and its position

k_B \ k_A	0.00	0.10	0.20	0.30	0.40	0.50	0.60	0.70	0.80	0.90	1.00
0.00	c = 5.00 d = 0.50	Sym.	Sym.	Sym.	Sym.	Sym.	Sym.	Sym.	Sym.	Sym.	Sym.
0.10	4.80 0.50	4.60 0.50	Sym.	Sym.	Sym.	Sym.	Sym.	Sym.	Sym.	Sym.	Sym.
0.20	4.60 0.51	4.40 0.50	4.20 0.50	Sym.	Sym.	Sym.	Sym.	Sym.	Sym.	Sym.	Sym.
0.30	4.40 1.35	4.20 0.51	4.00 0.50	3.80 0.50	Sym.	Sym.	Sym.	Sym.	Sym.	Sym.	Sym.
0.40	4.20 0.51	4.00 0.51	3.80 0.51	3.60 0.50	3.40 0.50	Sym.	Sym.	Sym.	Sym.	Sym.	Sym.
0.50	4.01 0.52	3.80 0.51	3.60 0.51	3.40 0.51	3.20 0.50	3.00 0.50	Sym.	Sym.	Sym.	Sym.	Sym.
0.60	3.81 0.52	3.61 0.52	3.40 0.52	3.20 0.51	3.00 0.51	2.80 0.50	2.60 0.50	Sym.	Sym.	Sym.	Sym.
0.70	3.61 0.53	3.41 0.52	3.21 0.52	3.00 0.52	2.80 0.51	2.60 0.51	2.40 0.50	2.20 0.50	Sym.	Sym.	Sym.
0.80	3.42 0.53	3.21 0.53	3.01 0.52	2.81 0.52	2.60 0.52	2.40 0.51	2.20 0.51	2.00 0.51	1.80 0.50	Sym.	Sym.
0.90	3.22 0.54	3.02 0.53	2.81 0.53	2.61 0.53	2.41 0.52	2.21 0.52	2.00 0.52	1.80 0.51	1.60 0.51	1.40 0.50	Sym.
1.00	3.03 0.54	2.82 0.54	2.62 0.54	2.42 0.53	2.21 0.53	2.01 0.53	1.81 0.52	1.60 0.52	1.40 0.51	1.20 0.51	1.00 0.50
1.10	2.83 0.55	2.63 0.55	2.43 0.54	2.22 0.54	2.02 0.54	1.81 0.54	1.61 0.53	1.41 0.53	1.20 0.52	/	/
1.20	2.64 0.55	2.44 0.55	2.23 0.55	2.03 0.55	1.82 0.55	1.62 0.54	1.42 0.54	/	/	/	/
1.30	2.45 0.56	2.25 0.56	2.04 0.56	1.84 0.56	1.63 0.56	/	/	/	/	/	/
1.40	2.27 0.57	2.06 0.57	1.86 0.57	/	/	/	/	/	/	/	/
1.50	2.08 0.58	/	/	/	/	/	/	/	/	/	/

With $\max. w = \frac{c}{384} \cdot \frac{q \cdot L^4}{E \cdot I}$ at $x_w = d \cdot L$

5.2 Determination of bending moment distribution

The bending moments at supports A and B can be expressed as follows:

$$M_A = -\frac{q \cdot L^2}{12} \cdot k_A \qquad (2)$$

$$M_B = -\frac{q \cdot L^2}{12} \cdot k_B \qquad (3)$$

where

$$k_A = \frac{m+6}{m+4+4 \cdot \frac{m}{n} + \frac{12}{n}}; \; k_B = \frac{n+6}{n+4+4 \cdot \frac{n}{m} + \frac{12}{m}}$$

and $n = \frac{S_{j,A} \cdot L}{E \cdot I}; \; m = \frac{S_{j,B} \cdot L}{E \cdot I}$

For $n \to \infty$ and $m \to 0$, then $k_A \to 1.5$ and $k_B \to 0$. This presents the standard case of a single-span beam with a hinged support on one side and rigid support on the other.

The well-known solution $M_A = -\frac{q \cdot L^2}{8}$ and $M_B = 0$ is obtained.

For a beam with rigid supports at both ends, then $k_A \to 1.0$ and $k_B \to 1.0$, and the solution is

$$M_A = M_B = -\frac{q \cdot L^2}{12}.$$

The vertical support reaction A as a function of k_A and k_B can be expressed as follows:

$$A = \frac{q \cdot L}{2} + \frac{q \cdot L}{12} \cdot \left(k_A - k_B\right) \qquad (4)$$

Table 5. Factor e for determining the natural frequency

k_B \ k_A	0.00	0.10	0.20	0.30	0.40	0.50	0.60	0.70	0.80	0.90	1.00
0.00 e =	1.00	Sym.	Sym.	Sym.	Sym.	Sym.	Sym.	Sym.	Sym.	Sym.	Sym.
0.10	1.02	1.04	Sym.	Sym.	Sym.	Sym.	Sym.	Sym.	Sym.	Sym.	Sym.
0.20	1.04	1.07	1.09	Sym.	Sym.	Sym.	Sym.	Sym.	Sym.	Sym.	Sym.
0.30	1.07	1.09	1.12	1.15	Sym.	Sym.	Sym.	Sym.	Sym.	Sym.	Sym.
0.40	1.09	1.12	1.15	1.18	1.22	Sym.	Sym.	Sym.	Sym.	Sym.	Sym.
0.50	1.12	1.15	1.18	1.22	1.25	1.30	Sym.	Sym.	Sym.	Sym.	Sym.
0.60	1.15	1.18	1.22	1.25	1.30	1.34	1.39	Sym.	Sym.	Sym.	Sym.
0.70	1.18	1.21	1.25	1.30	1.34	1.39	1.45	1.52	Sym.	Sym.	Sym.
0.80	1.21	1.25	1.29	1.34	1.39	1.45	1.52	1.59	1.68	Sym.	Sym.
0.90	1.25	1.29	1.34	1.39	1.45	1.52	1.59	1.68	1.79	1.91	Sym.
1.00	1.29	1.34	1.39	1.45	1.51	1.59	1.68	1.78	1.91	2.07	2.27
1.10	1.34	1.39	1.45	1.51	1.59	1.68	1.78	1.91	2.06	/	/
1.20	1.38	1.44	1.51	1.58	1.67	1.77	1.90	/	/	/	/
1.30	1.44	1.50	1.58	1.66	1.77	/	/	/	/	/	/
1.40	1.50	1.57	1.66	/	/	/	/	/	/	/	/
1.50	1.56	/	/	/	/	/	/	/	/	/	/

With $f_1 = e \cdot \frac{\pi^2}{2 \cdot \pi \cdot L^2} \cdot \sqrt{\frac{E \cdot I}{m}}$, with m = uniform mass

and the bending moment as a function of x:

$$M(x) = A \cdot x + M_A - \frac{1}{2} \cdot q \cdot x^2 \tag{5}$$

Using Eqs. (2) and (4) with Eq. (5), the following expression is derived for the bending moment as a function of x and the stiffness coefficients k_A and k_B:

$$M(x) = \frac{q \cdot L}{2} \cdot x + \frac{q \cdot L}{12} \cdot (k_A - k_B) \cdot x - \frac{q \cdot L^2}{12} \cdot k_A - \frac{1}{2} \cdot q \cdot x^2 \tag{6}$$

The position of the maximum bending moment can be calculated with M′(x) = 0, which leads to

$$M'(x) = 0 \Rightarrow \frac{q \cdot L}{2} + \frac{q \cdot L}{12} \cdot (k_A - k_B) - q \cdot x = 0 \Rightarrow \Rightarrow x = \frac{L}{2} + \frac{L}{12} \cdot (k_A - k_B) \tag{7}$$

Eq. (7) can be expressed in a dimensionless format:

$$b = \frac{x}{L} = \frac{1}{2} + \frac{1}{12} \cdot (k_A - k_B) \tag{8}$$

Using Eqs. (7) and (6), the maximum bending moment in the span M_{Span} can be expressed as

$$\max. M_{Span} = \frac{q \cdot L^2}{12} \cdot a \tag{9}$$

where $a = \frac{3}{2} + \frac{1}{2} \cdot (k_A - k_B) + \frac{1}{24} \cdot (k_A - k_B)^2 - k_A$

$$x_{max} = b \cdot L \tag{10}$$

Values for factors a and b, as a function of stiffness coefficients k_A and k_B, are given in Table 3.

5.3 Influence of semi-continuous joints on beam deflection

The beam deflection is expressed by the well-known linear differential equation

$$w''(x) = -\frac{M(x)}{E \cdot I} \tag{11}$$

After applying Eq. (5) in place of M(x), Eq. (11) takes the following form:

$$\begin{aligned} -E \cdot I \cdot w''(x) &= M(x) = A \cdot x + M_A - \frac{1}{2} \cdot q \cdot x^2 \\ -E \cdot I \cdot w'(x) &= A \cdot \frac{1}{2} \cdot x^2 + M_A \cdot x - \frac{1}{6} \cdot q \cdot x^3 + C_1 \\ -E \cdot I \cdot w(x) &= A \cdot \frac{1}{6} \cdot x^3 + M_A \cdot \frac{1}{2} \cdot x^2 - \frac{1}{24} \cdot q \cdot x^4 + C_1 \cdot x + C_2 \end{aligned} \tag{12}$$

Constants C_1 and C_2 are determined with the boundary conditions:

$$w(x = L) \Rightarrow C_1 = -\frac{1}{6} \cdot A \cdot L^2 - \frac{1}{2} \cdot M_A + \frac{1}{24} \cdot q \cdot L^3$$

$$w(x = 0) \Rightarrow C_2 = 0$$

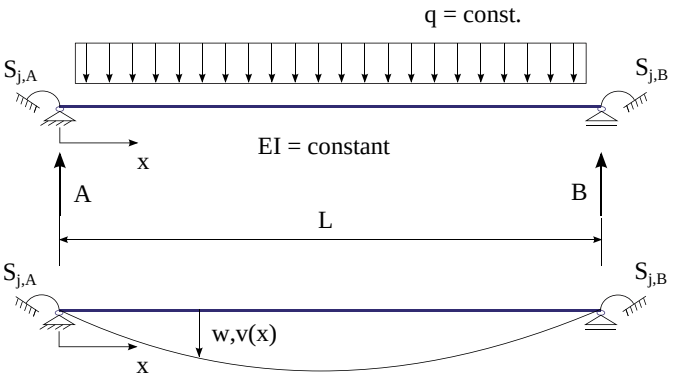

Fig. 8. Simply supported beam with rotational springs at the supports

Finally, the beam deflection as a function of the stiffness of the rotational springs is defined as follows:

$$-E \cdot I \cdot w(x) = \frac{1}{6} \cdot A \cdot \left(x^3 - L^2 \cdot x\right) + \frac{1}{2} \cdot M_A \cdot \left(x^2 - L \cdot x\right) - \frac{1}{24} \cdot q \cdot \left(x^4 - L^3 \cdot x\right) \quad (13)$$

$$-E \cdot I \cdot w(x) = \frac{1}{72} \cdot q \cdot \left(k_A - k_B + 6\right) \cdot \left(L \cdot x^3 - L^3 \cdot x\right) - \frac{1}{24} \cdot q \cdot k_A \cdot \left(L^2 \cdot x^2 - L^3 \cdot x\right) - \frac{1}{24} \cdot q \cdot \left(x^4 - L^3 \cdot x\right) \quad (14)$$

The design value and position of the maximal vertical deflection is of key interest for the designer. It is derived from

$$-E \cdot I \cdot w'(x) = \varphi(x) = 0 \Rightarrow A \cdot \frac{1}{2} \cdot x^2 + M_A \cdot x - \frac{1}{6} \cdot q \cdot x^3 + C_1 = 0 \quad (15)$$

This equation of the third order is solved by using the formulae from Cardan:

$$\varphi(x) = x^3 + x^2 \cdot \underbrace{\left[\frac{L}{4} \cdot \left(k_B - k_A\right) - \frac{3}{2} \cdot L\right]}_{r} + x \cdot \underbrace{\frac{L^2}{2} \cdot k_A}_{s} + \underbrace{\frac{L^3}{12} \cdot \left(3 - 2 \cdot k_A - k_B\right)}_{t} = 0 \quad (16)$$

Substituting x = y – r/3, the reduced form is obtained:

$$y^3 + p \cdot y + q = 0 \text{ with } p = \frac{3 \cdot s - r^2}{3} \text{ and } q = \frac{2 \cdot r^3}{27} - \frac{r \cdot s}{3} + t$$

The discriminant D can be expressed as

$$D = \left(\frac{p}{3}\right)^3 + \left(\frac{q}{2}\right)^2$$

For the given application range of the rotation ($0 \le x \le L$) and for the stiffness coefficients k_A and k_B ($0 \le k_A, k_B \le 1.5$), the discriminant is always $D \le 0$ and $p < 0$. Therefore, Eq. (15) has three real solutions. The solution gives the position of the maximum beam deflection and can be expressed as a factor d. By using the now known position of the maximum vertical beam deflection with Eq. (14), the value of the maximum deflection can be calculated. Hence, the maximum vertical beam deflection w can be calculated using

$$\max. w = \frac{c}{384} \cdot \frac{q \cdot L^4}{E \cdot I} \quad (17)$$

and the position of the maximum deflection with

$$x_w = d \cdot L \quad (18)$$

Pre-calculated values for factors c and d as a function of the stiffness coefficients k_A and k_B are given in Table 4.

5.4 Influence of semi-rigid joints on the natural frequency of the beam

The natural frequency of the beam is of significant interest for the structural engineer. Based on the differential equation of the harmonic vibration, a factor e, which allows a quick determination of the natural frequency, is given in Table 5.

$$v(x) = C_1 \cdot \cos\left(\lambda \cdot \frac{x}{L}\right) + C_2 \cdot \sin\left(\lambda \cdot \frac{x}{L}\right) + C_3 \cdot \cosh\left(\lambda \cdot \frac{x}{L}\right) + C_4 \cdot \sinh\left(\lambda \cdot \frac{x}{L}\right) \quad (19)$$

$$v'(x) = \frac{\lambda}{L} \cdot \left[-C_1 \cdot \sin\left(\lambda \cdot \frac{x}{L}\right) + C_2 \cdot \cos\left(\lambda \cdot \frac{x}{L}\right) + C_3 \cdot \sinh\left(\lambda \cdot \frac{x}{L}\right) + C_4 \cdot \cosh\left(\lambda \cdot \frac{x}{L}\right)\right] \quad (20)$$

$$v''(x) = \frac{\lambda^2}{L^2} \cdot \left[-C_1 \cdot \cos\left(\lambda \cdot \frac{x}{L}\right) - C_2 \cdot \sin\left(\lambda \cdot \frac{x}{L}\right) + C_3 \cdot \cosh\left(\lambda \cdot \frac{x}{L}\right) + C_4 \cdot \sinh\left(\lambda \cdot \frac{x}{L}\right)\right] \quad (21)$$

$$v'''(x) = \frac{\lambda^3}{L^3} \cdot \left[C_1 \cdot \sin\left(\lambda \cdot \frac{x}{L}\right) - C_2 \cdot \cos\left(\lambda \cdot \frac{x}{L}\right) + C_3 \cdot \sinh\left(\lambda \cdot \frac{x}{L}\right) + C_4 \cdot \cosh\left(\lambda \cdot \frac{x}{L}\right)\right] \quad (22)$$

The constants are determined with the boundary conditions:

$$v(x = 0) = 0 \Rightarrow C_1 + C_3 = 0$$

$$v(x = L) = 0 \Rightarrow C_1 \cdot \left(\cos\lambda - \cosh\lambda\right) + C_2 \cdot \sin\lambda + C_4 \cdot \sinh\lambda = 0$$

$$-v''(x = 0) + \frac{n}{L} \cdot v'(x = 0) = 0 \Rightarrow 2 \cdot C_1 \cdot \lambda + \frac{S_{j,A} \cdot L}{E \cdot I} \cdot C_2 + \frac{S_{j,A} \cdot L}{E \cdot I} \cdot C_4 = 0$$

$$-v''(x=L) - \frac{m}{L}\cdot v'(x=L) = 0 \Rightarrow C_1\cdot[\lambda\cdot(\cos\lambda+\cosh\lambda) + \frac{S_{j,B}\cdot L}{E\cdot I}\cdot(\sin\lambda+\sinh\lambda)] + C_2\cdot\left[\lambda\cdot\sin\lambda - \frac{S_{j,B}\cdot L}{E\cdot I}\cdot\cos\lambda\right] - C_4\cdot\left[\frac{S_{j,B}\cdot L}{E\cdot I}\cdot\cosh\lambda + \lambda\cdot\sinh\lambda\right] = 0$$

which leads to the following linear equation system:

$$\mathbf{B}\cdot\mathbf{C} = \mathbf{0} \text{ mit} \quad (23)$$

$$\mathbf{B} = \begin{pmatrix} b_{11} & b_{12} & b_{13} \\ b_{21} & b_{22} & b_{23} \\ b_{31} & b_{32} & b_{33} \end{pmatrix} \text{ und } \mathbf{C} = \begin{pmatrix} C_1 \\ C_2 \\ C_4 \end{pmatrix}$$

$b_{11} = \cos\lambda - \cosh\lambda$
$b_{12} = \sin\lambda$
$b_{13} = \sinh\lambda$
$b_{21} = 2\lambda$
$b_{22} = b_{23} = n$
$b_{31} = \lambda(\cos\lambda + \cosh\lambda) + m(\sin\lambda + \sinh\lambda)$
$b_{32} = \lambda\sin\lambda - m\cdot\cos\lambda$
$b_{33} = -m\cosh\lambda - \lambda\sinh\lambda$

The equation system is solved if the determinant of matrix **B** = 0. The lowest value for λ_i for which the above equation system is solved (the trivial solution $\lambda = 0$ is forbidden) is required. The determinant of matrix **B** is expressed with

$$\mathrm{Det}(B) = n\cdot m\cdot(1-\cos\lambda\cdot\cosh\lambda) + \lambda\cdot n\cdot(\cosh\lambda\cdot\sin\lambda - \cos\lambda\cdot\sinh\lambda) + \lambda\cdot m\cdot(\cosh\lambda\cdot\sin\lambda - \cos\lambda\cdot\sinh\lambda) + 2\cdot\lambda^2\cdot\sin\lambda\cdot\sinh\lambda = 0 \quad (24)$$

Solutions for λ as a function of stiffness coefficients k_A and k_B are given in Table 5.

The natural frequency can be calculated with

$$f_1 = \frac{\lambda_i^2}{2\cdot\pi\cdot L^2}\cdot\sqrt{\frac{E\cdot I}{m}} = e\cdot\frac{\pi^2}{2\cdot\pi\cdot L^2}\cdot\sqrt{\frac{E\cdot I}{m}} \quad (25)$$

where m = uniformly distributed constant mass.

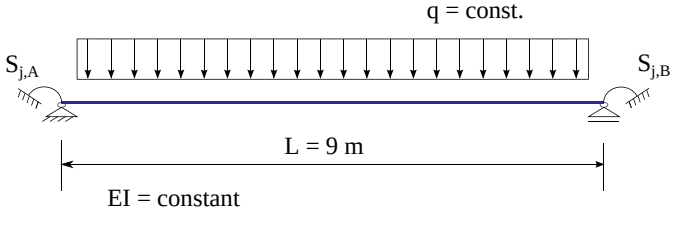

Fig. 9a. Application example – structural system and loading

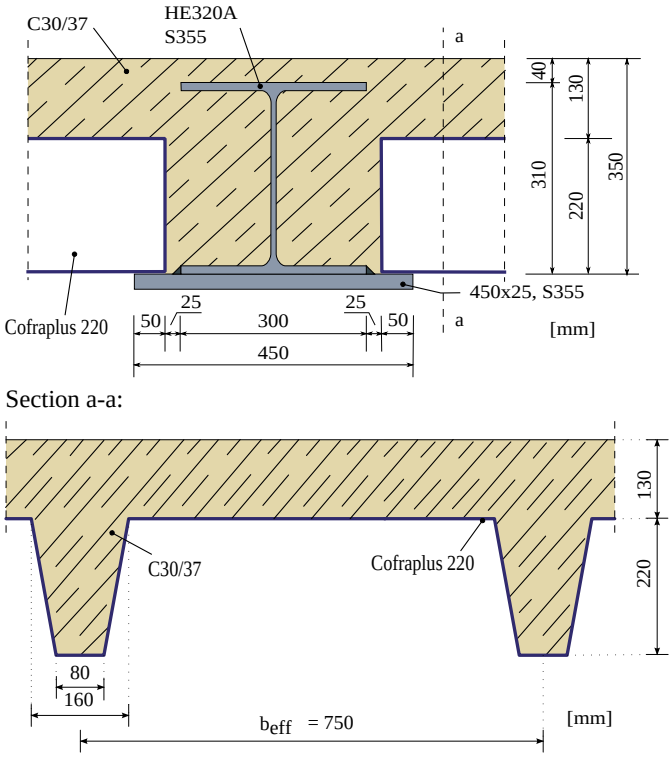

Fig. 9b. Application example – SFB cross-section with slab

Note: As Eq. (24) is non-algebraic, it had to be solved by numerical iteration. Therefore, the given values for the factor e are an approximation. The given factors a, b, c and d (described in the previous sections) are precise results, rounded to two digits.

6 Application example – single-span slim-floor beam with semi-continuous joints

6.1 Structural system and loading

The use of semi-continuous joints using elastic–plastic global analysis is demonstrated for a single-span slim-floor beam (SFB) with a beam span L = 9.00m and a beam distance a = 8.10 m (axis-to-axis). The beam is loaded with a uniformly distributed constant load q, has a constant bending stiffness EI and it is symmetrically supported in an internal bay, see Fig. 9a. The SFB cross-section consists of an HE320A hot-rolled section in grade S355 and a welded bottom plate, see Fig. 9b. The SFB section has an inertia I_y = 39560cm^4 with $z_{el,top}$ = 23.445 cm (measured from top of upper flange downwards); possible participation of the concrete is not taken into account. The slab consists of Cofraplus 220 metal decking with 13 cm in situ concrete [7]. It is shown that the use of semi-continuous joints leads to an economical beam design for the ultimate limit state (ULS) and to improved deflection and vibration behaviour of the beam at the serviceability limit state (SLS).

Safety factors: $\gamma_{M0} = 1.00$; $\gamma_{M1} = 1.00$; $\gamma_{M2} = 1.25$
Yield strength of hot-rolled section, HE320A, S355: $f_{yd} = 355$ N/mm^2
Yield strength of bottom plate, 450 × 25 mm, S355: $f_{yd} = 345$ N/mm^2

Elastic bending resistance of SFB cross-section:

$$M_{el,Rd} = \frac{f_{yd} \cdot I_y}{z_{el,top}} = \frac{35.5\ kN/cm^2 \cdot 39560\ cm^4}{23.445\ cm}$$

$$= 599\ kNm$$

Plastic bending resistance of SFB cross-section: $M_{pl,Rd}$ = 732 kNm with z_{pl} = 30.75 cm from top of upper flange downwards (by hand calculation).

The beam-to-column joints are realized as end-plate connections with a rotational stiffness $S_{j,A} = S_{j,B}$.

Load assumptions:
Cofraplus 220 with 13 cm concrete: $g_{C+220} = 4.29\ kN/m^2$
Additional dead load: $\Delta g = 1.20\ kN/m^2$
Self-weight of SFB with concrete encasement:
$g_{SFB} = 1.82\ kN/m + 2.75\ kN/m = 4.57\ kN/m$
Dead load (slab + beam, self-weight):

$$\Sigma g_k = [1.1 \cdot 4.29\ kN/m^2 \cdot (8.10 - 0.45 + 2 \cdot 0.05)\ m + 1.1 \cdot 1.20\ kN/m^2 \cdot 8.10\ m] + 4.57\ kN/m = 51.83\ kN/m$$

Live load (category B1, office use, $\psi_0 = 0.70$): 2.00 kN/m²
Partitions: 1.20 kN/m²
$\Sigma q_k = 1.1 \cdot (2.00 + 1.20)\ kN/m^2 \cdot 8.10\ m = 28.51\ kN/m$

Reduction factor: $\alpha_A = \frac{5}{7} \cdot \psi_0 + \frac{10\ m^2}{9 \cdot 8.10\ m^2} = 0.64$

Reduced live load:
$q'_k = \Sigma q_k \cdot \alpha_A = 28.51\ kN/m \cdot 0.64 = 18.17\ kN/m$

The additional load on the beam due to continuity of the slab – perpendicular to beam span – is taken into account by a factor of 1.10.

Load combinations:
Total characteristic load: $E_k = q_{SLS} = \Sigma g_k + q'_k = 51.83\ kN/m = 18.17\ kN/m = 70.0\ kN/m$
Design load: $E_d = q_{ULS} = 1.35 \cdot \Sigma g_k + 1.50 \cdot q'_k = 1.35 \cdot 51.83\ kN/m + 1.50 \cdot 18.17\ kN/m = 97.2\ kN/m$

6.2 Section classification

Cross-section at mid-span – pure bending, positive bending moment:
Upper flange in compression:

$$9 \cdot \varepsilon = 9 \cdot \sqrt{\frac{235}{355}} = 7.32 < \frac{c}{t} = \frac{0.5 \cdot (300 - 9 - 2 \cdot 27)}{15.5}$$

$$= \frac{118.5}{15.5} = 7.65 < 8.14 = 10 \cdot \sqrt{\frac{235}{355}} = 10 \cdot \varepsilon \Rightarrow \text{class 2}$$

Web in compression:

$$\frac{c}{t} = \frac{310 - 2 \cdot 15.5 - 2 \cdot 27}{9} = \frac{225}{9}$$

$$= 25.0 < 58.58 = 72 \cdot \sqrt{\frac{235}{355}} = 72 \cdot \varepsilon \Rightarrow \text{class 1}$$

⇒ At mid-span the SFB section is classified as a class 2 section. A class 2 section can develop its plastic cross-sectional resistance, but has not enough rotational capacity to allow for a plastic hinge.

Cross-section at supports – pure bending, negative bending moment:
Edge of bottom plate in compression:

$$\frac{c}{t} = \frac{75}{25} = 3.00 < 7.43 = 9 \cdot \sqrt{\frac{235}{345}} = 9 \cdot \varepsilon \Rightarrow \text{class 1}$$

Bottom plate + lower flange in compression:

$$\frac{c}{t} = \frac{0.5 \cdot (300 - 9 - 2 \cdot 27)}{25.0 + 15.5} = \frac{118.5}{40.5} = 2.93 < 7.43$$

$$= 9 \cdot \sqrt{\frac{235}{355}} = 9 \cdot \varepsilon \Rightarrow \text{class 1}$$

⇒ At the supports the SFB section is classified as a class 1 section, which can form a plastic hinge with the rotational capacity required from plastic analysis without a reduction in the resistance.

6.3 Semi-continuous beam-to-column joint

The design of the joint is not presented in detail in this article. The joint can be designed using standard software or even by hand calculation; reference is made to [1]. The joint is designed as semi-continuous with an extended end plate, see Fig. 10. Both beam ends are connected symmetrically to the columns with end plates ($S_{j,A} = S_{j,B}$, n = m, $k_A = k_B$).

The design moment–rotation characteristic of the joint is presented in Fig. 11a and was calculated according to [1]. The initial stiffness $S_{j,ini}$ is within the boundaries for a semi-rigid joint (see also Fig. 5). Its design moment resistance $M_{j,Rd}$ = 360 kNm is within the limits given in Fig. 6 for a partial-strength joint ($0.25 \cdot M_{pl,Rd} \le M_{j,Rd} \le M_{pl,Rd}$ with $M_{pl,Rd} = M_{b,pl,Rd}$ = 732 kNm). Therefore the joint is classified as semi-rigid and partial-strength and is modelled in design as semi-continuous joint.

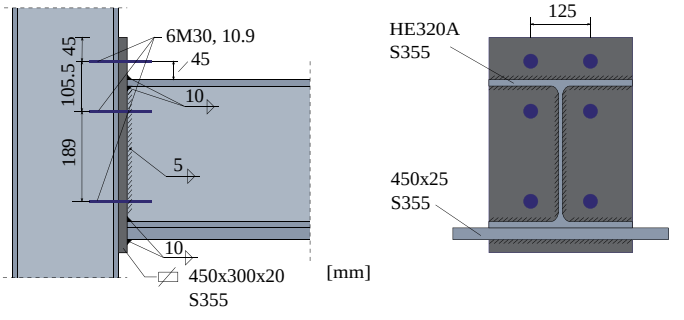

Fig. 10. Application example – basic components of semi-continuous joint

For the following analysis of the SFB for SLS and ULS, a tri-linear approximation of the moment–rotation characteristic is used in accordance with 5.1.1(4) of [1], see Fig. 11b. It is divided into three areas:

- An elastic area for a joint rotation ϕ_j within the range $0 \le \phi_j \le \phi_{j,el}$
- A second area for a joint rotation ϕ_j within the range $\phi_{j,el} \le \phi_j \le \phi_{Xd}$
- A plastic area for a joint rotation ϕ_j within the range $\phi_{Xd} \le \phi_j \le \phi_{Cd}$

Note: Using Eq. (1) and Table 2 of section 4.3, an approximate joint stiffness $S_{j,app}$ could be calculated as follows:

$$S_{j,app} = \frac{E \cdot z^2 \cdot t_{fc}}{C} = \frac{210000\ \text{MN/m}^2 \cdot (0.307\ \text{m})^2 \cdot 0.0215\ \text{m}}{7.5}$$
$$= 56.7\ \text{MNm/rad} = 56.7\ \text{kNm/mrad}$$

Based on the given SFB section, the structural system and the design moment–rotation characteristic (Fig. 11b), the corresponding load levels $q_{j,el}$ and $q_{j,Rd}$ are calculated for the joint rotations $\phi_{j,el}$ and ϕ_{Xd}.

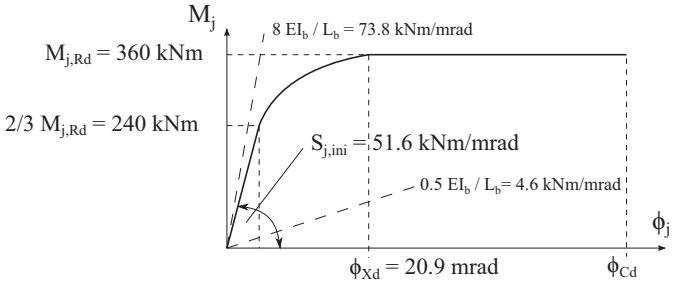

Fig. 11a. Application example – design moment–rotation characteristic of semi-continuous joint

Calculation of $q_{j,el}$

Up to a bending moment $M_{j,Ed} \le \frac{2}{3} \cdot M_{j,Rd}$, the initial joint stiffness $S_{j,ini}$ can be used in the calculation, see 5.1.2(3) in [1].

$$\frac{2}{3} \cdot M_{j,Rd} = \frac{2}{3} \cdot 360\ \text{kNm} = 240\ \text{kNm}$$
$$\Rightarrow S_{j,ini} = 51.6\ \text{MNm/rad}$$

Using the equations given in section 5, it is possible to calculate the values for n = m and $k_A = k_B$:

$$n = m = \frac{S_{j,ini} \cdot L}{E \cdot I} = \frac{51.6\ \text{MNm/rad} \cdot 9.0\ \text{m}}{210000\ \text{MN/m}^2 \cdot 39560 \cdot 10^{-8}\text{m}^4}$$
$$= 5.59\ \frac{[-]}{\text{rad}}$$

$$k_A = k_B = \frac{m+6}{m+4+4 \cdot \frac{m}{n} + \frac{12}{n}} = \frac{5.59+6}{5.59+4+4 \cdot \frac{5.59}{5.59} + \frac{12}{5.59}}$$
$$= 0.74$$

And using Eq. (2) we get $q_{j,el}$:

$$\frac{2}{3} \cdot M_{j,Rd} = 240\ \text{kNm} = \frac{q_{j,el} \cdot L^2}{12} \cdot k_A = \frac{q_{j,el} \cdot (9\ \text{m})^2}{12} \cdot 0.74$$
$$\Rightarrow q_{j,el} = 48.0\ \text{kN/m}$$

Calculation of $q_{j,Rd}$

For a bending moment $M_{j,Ed}$ in the range

$$\frac{2}{3} \cdot M_{j,Rd} < M_{j,Ed} \le M_{j,Rd}$$

we use the joint stiffness $S_{j,2}$ = 7.4 MNm/rad, see Fig. 11b.

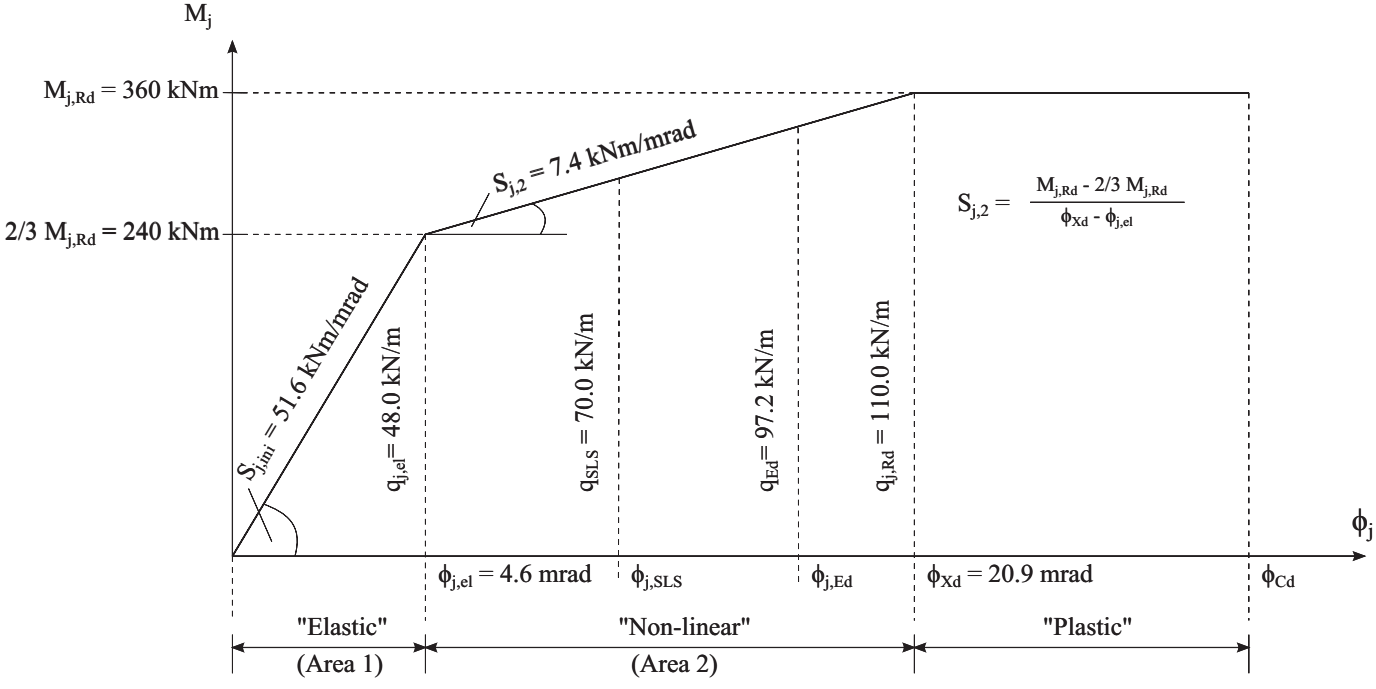

Fig. 11b. Application example – tri-linear approximation of design moment–rotation characteristic

First, factors $n_2 = m_2$ and $k_{A,2}$ and $k_{B,2}$ have to be calculated:

$$n_2 = m_2 = \frac{S_{j,2} \cdot L}{E \cdot I} = \frac{7.4\ \text{MNm/rad} \cdot 9.0\ \text{m}}{210000\ \text{MN/m}^2 \cdot 39560 \cdot 10^{-8}\text{m}^4} = 0.80\ \frac{[-]}{\text{rad}}$$

$$k_{A,2} = k_{B,2} = \frac{m_2 + 6}{m_2 + 4 + 4 \cdot \frac{m_2}{n_2} + \frac{12}{n_2}} = \frac{0.80 + 6}{0.80 + 4 + 4 \cdot \frac{0.80}{0.80} + \frac{12}{0.80}} = 0.29$$

Using Eq. (2) we get

$$M_{j,Rd} - \frac{2}{3} \cdot M_{j,Rd} = 360\ \text{kNm} - 240\ \text{kNm} = 120\ \text{kNm}$$

$$= \frac{\Delta q \cdot L^2}{12} \cdot k_A = \frac{\Delta q \cdot (9\ \text{m})^2}{12} \cdot 0.29$$

$$\Rightarrow \Delta q = 62.0\ \text{kN/m}$$

and $q_{j,Rd} = q_{j,el} + \Delta q = 48.0\ \text{kN/m} + 62.0\ \text{kN/m} = 110.0\ \text{kN/m}$

6.4 Beam design for SLS

The total vertical beam deflection and the natural frequency of the SFB are determined by using the equations and tables in section 5. In the absence of a more precise method for defining the joint stiffness, the tri-linear design moment–rotation characteristic of Fig. 11b is used, which represents a sufficiently precise approximation of the real joint behaviour.

Total characteristic load:

$$E_k = \Sigma g_k + q'_k = 51.83\ \text{kN/m} + 18.17\ \text{kN/m} = 70.0\ \text{kN/m}$$

Load combination for beam deflection at mid-span:

$$q_{SLS} = 1.0 \cdot \Sigma g_k + 1.0 \cdot q'_k = 1.0 \cdot 51.83\ \text{kN/m} + 1.0 \cdot 18.17\ \text{kN/m} = 70.0\ \text{kN/m}$$

Load combination for natural frequency:

$$q_{Hz} = 1.0 \cdot \Sigma g_k + 0.20 \cdot q'_k = 1.0 \cdot 51.83\ \text{kN/m} + 1.0 \cdot 18.17\ \text{kN/m} = 55.5\ \text{kN/m}$$

Calculation of SFB deflection at mid-span:
As shown in Fig. 11b, the load q_{SLS} is in "area 2" ($q_{j,el} \le q_{SLS} = 70.0\ \text{kN/m} \le q_{j,Rd}$), so the deflection w_{SLS} has to be calculated in two steps.

Step 1 – deflection w_{el} with $q_{j,el}$:
For $k_A = k_B = 0.74$, factor c is taken from Table 4: c = 2.04 (by linear interpolation).

Deflection w_{el} is calculated using Eq. (17):

$$\Rightarrow w_{el} = \frac{c}{384} \cdot \frac{q_{j,el} \cdot L^4}{E \cdot I} = \frac{2.04}{384} \cdot \frac{48.0 \cdot 10^{-2}\ \text{kN/cm} \cdot (900\ \text{cm})^4}{21000\ \text{kN/cm}^2 \cdot 39560\ \text{cm}^4} = 2.01\ \text{cm}$$

Step 2 – additional deflection Δw with Δq_{SLS}:
Taking the load $\Delta q_{SLS} = q_{SLS} - q_{j,el} = 70\ \text{kN/m} - 48\ \text{kN/m} = 22\ \text{kN/m}$, a deflection Δw is calculated using the joint stiffness $S_{j,2} = 7.4$ kNm/mrad, see Fig. 11b.

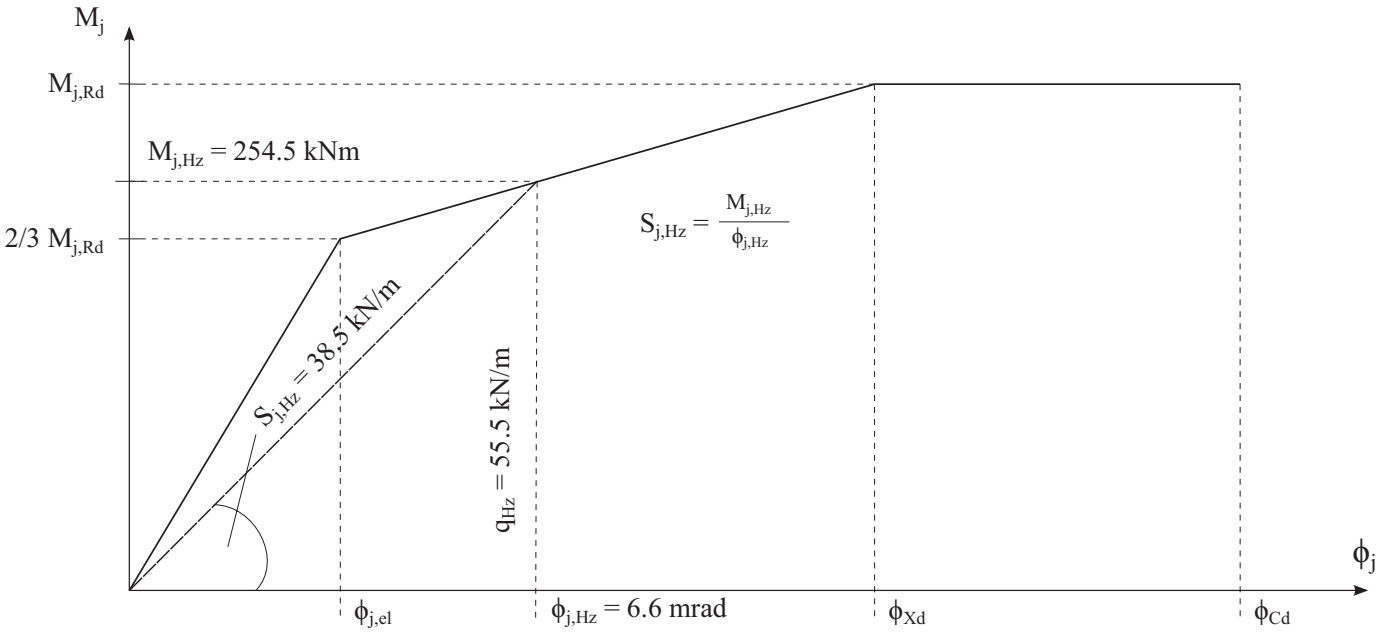

Fig. 12. Application example – idealized joint stiffness for vibration analysis $S_{j,Hz}$

With $k_{A,2} = k_{B,2} = 0.29$, factor c_2 is determined with Table 4: $c_2 = 3.84$ (by linear interpolation).
A deflection Δw is calculated using Eq. (17):

$$\Rightarrow \Delta w = \frac{c_2}{384} \cdot \frac{\Delta q_{SLS} \cdot L^4}{E \cdot I}$$

$$= \frac{3.84}{384} \cdot \frac{22.0 \cdot 10^{-2}\ \text{kN/cm} \cdot (900\ \text{cm})^4}{21000\ \text{kN/cm}^2 \cdot 39560\ \text{cm}^4}$$

$$= 1.74\ \text{cm}$$

which leads to the following total vertical deflection of the SFB at mid-span:

$w_{SLS} = w_{el} + \Delta w = 2.01\ \text{cm} + 1.74\ \text{cm} = 3.75\ \text{cm} \approx L/240 < L/200 \Rightarrow$ The deflection is within acceptable limits.

Note: With simple, hinged beam-to-column joints, the beam deflection at mid-span would be:

$$\Rightarrow w = \frac{5}{384} \cdot \frac{q_{SLS} \cdot L^4}{E \cdot I} = \frac{5}{384} \cdot \frac{70 \cdot 10^{-2}\ \text{kN/cm} \cdot (900\ \text{cm})^4}{21000\ \text{kN/cm}^2 \cdot 39560\ \text{cm}^4}$$

$$= 7.20\ \text{cm},$$

which is 1.92 times the deflection of the semi-continuous beam!

A basic assumption of the calculation of the beam deflection is an elastic material behaviour; the strains in the cross-section do not exceed the yield strain. To verify this assumption, the bending moment of the joint $M_{j,SLS}$ at SLS and the bending moment at mid-span M_{SLS} are calculated and compared with the elastic bending resistance of the SFB cross-section:

$$M_{j,SLS} = \frac{q_{j,el} \cdot L^2}{12} \cdot k_A + \frac{\Delta q_{SLS} \cdot L^2}{12} \cdot k_{A,2}$$

$$= \frac{2}{3} \cdot M_{j,Rd} + \frac{\Delta q_{SLS} \cdot L^2}{12} \cdot k_{A,2}$$

$$= \frac{2}{3} \cdot 360\ \text{kNm} + \frac{22\ \text{kN/m} \cdot (9\ \text{m})^2}{12} \cdot 0.29$$

$$= 240\ \text{kNm} + 43\ \text{kNm} = 283\ \text{kNm}$$

$$M_{SLS} = \frac{q_{SLS} \cdot L^2}{8} - M_{j,SLS} = \frac{70\ \text{kN/m} \cdot (9\ \text{m})^2}{8} - 283\ \text{kNm}$$

$$= 426\ \text{kNm} < M_{el,Rd} = 599\ \text{kNm}$$

$\Rightarrow$ The SFB cross-section remains fully elastic at SLS, the assumption is correct.

Calculation of the natural frequency of the SFB
The natural frequency of the SFB is determined based on the equations in section 5. The load q_{Hz} is in "area 2" ($q_{j,el} \le q_{Hz} = 55.5\ \text{kN/m} \le q_{j,Rd}$), and so an idealized joint stiffness $S_{j,Hz}$ is used, see Fig. 12. For q_{Hz}, the corresponding values of the joint rotation $\Phi_{j,Hz}$ and the bending moment $M_{j,Hz}$ are: $\Phi_{j,Hz} = 6.6$ mrad and $M_{j,Hz} = 254.5$ kNm $\Rightarrow S_{j,Hz} = M_{j,Hz}/\Phi_{j,Hz} = 254.5\ \text{kNm} / 6.6\ \text{mrad} = 38.5\ \text{kNm/mrad}$

$$n_{Hz} = m_{Hz} = \frac{S_{j,Hz} \cdot L}{E \cdot I}$$

$$= \frac{38.5\ \text{MNm/rad} \cdot 9.0\text{m}}{210000\ \text{MN/m}^2 \cdot 39560 \cdot 10^{-8}\text{m}^4} = 4.17\ \frac{[-]}{\text{rad}}$$

$$k_{A,Hz} = k_{B,Hz} = \frac{m_{Hz} + 6}{m_{H2} + 4 + 4 \cdot \frac{m_{Hz}}{n_{Hz}} + \frac{12}{n_{Hz}}}$$

$$= \frac{4.17 + 6}{4.17 + 4 + 4 \cdot \frac{4.17}{4.17} + \frac{12}{4.17}} = 0.68$$

From Table 5 we obtain $e = 1.49$ (by linear interpolation).

Using Eq. (25), the natural frequency can be calculated as follows:

$$f_1 = e \cdot \frac{\pi^2}{2 \cdot \pi \cdot L^2} \cdot \sqrt{\frac{E \cdot I}{m}} = 1.49 \cdot \frac{\pi^2}{2 \cdot \pi \cdot (9\ \text{m})^2} \cdot$$

$$\sqrt{\frac{21000\ \text{kN/m}^2 \cdot 39560\ \text{cm}^4 \cdot 10^{-4}}{55.5\ \text{kN/m}/9.81\ \text{m/s}^2}}$$

$$= 3.50\ \text{Hz} > 2.60\ \text{Hz}$$

The value of 2.60 Hz as a minimum acceptable natural frequency of the floor beams is found in [8]. Even though the natural frequency is commonly used to assess floor vibrations, the authors recommend using more precise methods that take into account the natural frequency of the whole floor and its modal mass. For further information see [9] and [10].

Note: With simple, hinged beam-to-column joints, the natural frequency of the SFB would be only 2.35 Hz!

6.5 Beam design for ULS

Design checks for bending and shear with semi-continuous joints
Based on the simplified tri-linear design moment–rotation characteristic given in Fig. 11b and a design load level $q_{j,el} < q_{Ed} = 97.2\ \text{kN/m} < q_{j,Rd}$, the bending moment at the joint $M_{j,Ed}$ and the one at mid-span M_{Ed} are calculated as follows:

$$M_{j,Ed} = \frac{q_{j,el} \cdot L^2}{12} \cdot k_A + \frac{(q_{Ed} - q_{j,el}) \cdot L^2}{12} \cdot k_{A,2}$$

$$= \frac{48\ \text{kN/m} \cdot (9\ \text{m})^2}{12} \cdot 0.74$$

$$+ \frac{(97.2 - 48)\text{kN/m} \cdot (9\ \text{m})^2}{12} \cdot 0.29$$

$$= 240\ \text{kNm} + 96\ \text{kNm} = 336\ \text{kNm} < M_{j,Rd}$$

$$M_{Ed} = \frac{q_{Ed} \cdot L^2}{8} - M_{j,Ed} = \frac{97.2\ \text{kN/m} \cdot (9\ \text{m})^2}{8} - 336\ \text{kNm}$$

$$= 984\ \text{kNm} - 336\ \text{kNm} = 648\ \text{kNm}$$

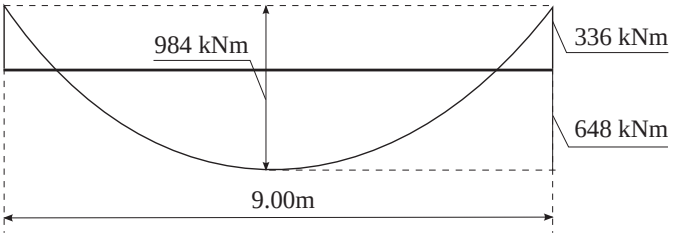

Fig. 13. Application example – bending moment distribution for ULS

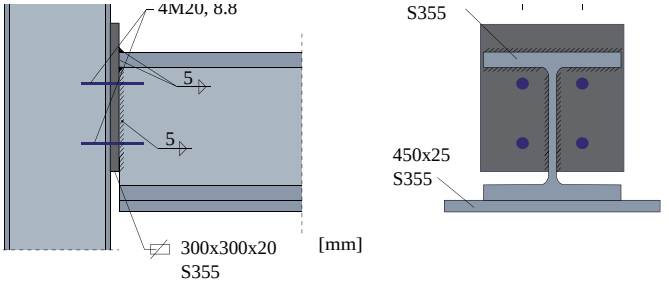

Fig. 14. Application example – nominally pinned joint configuration

which leads to the bending moment distribution presented in Fig. 13.

Verification of the SFB cross-section for bending at mid-span:

$$M_{Ed} = 648\text{kNm} \le M_{pl,Rd} = 732 \text{ kNm}$$
$$\Rightarrow \text{Verification is fulfilled!}$$

Note: With simple beam-to-column joints, the bending moment at mid-span M_{Ed} would exceed the bending resistance $M_{pl,Rd}$ of the cross-section:

$$M_{Ed} = 984 \text{ kNm} > M_{pl,Rd} = 732 \text{ kNm!}$$

Verification of the SFB cross section at the supports:

Bending: $M_{j,Rd} = 336 \text{ kNm} \le M_{pl,Rd} = 732 \text{ kNm}$

Shear:

$$V_{Ed} = q_{Ed} \cdot L/2 = 97.2 \text{ kN/m} \cdot 9 \text{ m}/2$$
$$= 437.4 \text{ kN} \le V_{pl,Rd} = \frac{A_{vz}}{\sqrt{3}} \cdot f_{yd}$$
$$= \frac{41.13 \text{ cm}^2}{\sqrt{3}} \cdot 35.5 \text{ kN/cm}^2 = 843 \text{ kN}$$

$\Rightarrow$ Verification is fulfilled!

With a load ratio $V_{Ed}/V_{pl,Rd}$ = 437.4 kN/843 kN = 0.52 > 0.50, the bending resistance has to be reduced due to the presence of a shear force. According to 6.2.8 of [11], this may be done by reducing the yield strength of the shear area by

Table 6. Application example – cost comparison: simple joints vs. semi-continuous joints

Joint Type / Component	Simple	Semi-continuous	Cost Difference* €/SFB
Hot Rolled Section (Grade S355)	HE280M	HE320A	– 480 €
Weld size (Endplate to flanges only)	5 mm	10 mm	+ 100 €
Endplate (Grade S355)	300 × 300 × 20	450 × 300 × 20	+ 20
Bolts	4 M 20, 8.8	6 M 30, 10.9	+ 60 €
Total ΔCost:			**– 300 €**
⇒ Beam Design with semi-continuous joints is **300 € cheaper** (per 9 m SFB)!			

* Estimated cost based on 2015 price level, including erection.

$$f_{yd,V} = \left[1 - \left(\frac{2 \cdot V_{Ed}}{V_{pl,Rd}} - 1\right)^2\right] \cdot f_{yd}$$
$$= \left[1 - \left(\frac{2 \cdot 437.4 \text{ kN}}{843 \text{ kN}} - 1\right)^2\right] \cdot 35.5 \text{ kN/cm}^2$$
$$= 35.45 \text{ kN/cm}^2$$

As this reduction in the yield strength is < 1 %, it is neglected in this example.

The SFB cross-section is not plastified at the supports. At mid-span it is partially plastified, but there is still no development of a plastic hinge; therefore, the classification of the cross-section in class 2 is sufficient for the chosen design method.

Rotational capacity of the joint

Elastic–plastic global analysis was used in the given example. The joint is not located at the position of a plastic hinge, and the acting design moment does not reach the value of the design moment resistance, $M_{j,Ed} < M_{j,Rd}$. Therefore, the rotation ϕ_{Ed} does not reach ϕ_{Xd} and the rotational capacity of the joint does not have to be checked.

6.6 Economic evaluation of semi-continuous joints

This section compares the cost of the SFB designed with semi-continuous joints with a beam design using simple joints. The design of the simply supported SFB was carried out with the software [12] and was based on the same assumptions as the design of the semi-continuous SFB (same load assumptions and L = 9.0 m, a = 8.10 m, h_{Slab} = 350 mm). The basic components of the simple joint are shown in Fig. 14. The cost difference for the basic components is presented in Table 6. Only the direct costs of the non-identical parts are given; the possible influence of the joint design on the foundations, columns etc. was not taken into account.

7 Conclusion and outlook

This article outlines the advantage of semi-continuous beam-to-column joints for the design of single-span beams (with constant inertia and subjected to a uniformly distributed constant load) at ULS and SLS. Factors for use in combination with standard design formulae were derived analytically. They allow the structural engineer to determine the influence of the joint stiffness on the beam deflection, its natural frequency and the distribution of the bending moment quickly and easily. Further, the application is shown in a design example for a slim-floor beam (SFB), which shows the economic potential of semi-continuous joints. Overall, such joints lead to a more economic, more sustainable structure. The influence of semi-continuous joints on the design of single-span beams with partially constant inertia will be investigated in a second article.

References

[1] CEN/TC250: Eurocode 3: Design of steel structures – Part 1-8: Design of joints, European Commission.

[2] *Braun, M., Hechler, O., Obiala, R.*: Untersuchungen zur Verbundwirkung von Betondübeln. Stahlbau, 83 (2014), No. 5. DOI:10.1002/stab.201410154

[3] Deutsches Institut für Bautechnik: Allgemeine bauaufsichtliche Zulassung – CoSFB-Betondübel. ArcelorMittal Belval & Differdange S.A., approval No. Z-26.4-59, Berlin, 2014.

[4] *Ungermann, D., Weynand, K., Jaspart, J.-P., Schmidt, B.*: Momententragfähige Anschlüsse mit und ohne Steifen. Stahlbau-Kalender 2005, *Kuhlmann, U.* (ed.), Ernst & Sohn, Berlin, ISBN 3-433-01721-2.

[5] *Jaspart, J.-P., Demonceau, J.-F.*: European Design Recommendations for simple joints in steel structures. ArGEnCo Dept., Liège University.

[6] *Maquoi, R., Chabrolin, B.*: Frame Design including joint behaviour. European Commission, contract No. 7210-SA/212/320, 1998.

[7] Deutsches Institut für Bautechnik: Allgemeine bauaufsichtliche Zulassung – ArcelorMittal Systemdecke Cofraplus 220, approval No. Z-26.1-55, Berlin, 2013.

[8] AFNOR: National annex to NF EN 1993-1-1, Eurocode 3: Design of steel structures – Part 1-1: General rules and rules for buildings.

[9] *Sedlacek, G.*, et al.: Generalization of criteria for floor vibrations for industrial, office, residential and public building and gymnastic halls. European Commission, final report, 2006, EUR 21972 EN, ISBN 92-79-01705-5.

[10] *Hicks, S., Peltonen, S.*: Design of slim-floor construction for human induced vibrations. Steel Construction, 8 (2015), No. 2. DOI:10.1002/stco.201510015

[11] CEN/TC250: Eurocode 3: Design of steel structures – Part 1-1: General rules and rules for buildings, European Commission.

[12] CTICM France, ArcelorMittal R&D: ArcelorMittal Beam Calculator (ABC), version 3.30, ArcelorMittal Belval & Differdange S.A. http://sections.arcelormittal.com/download-center/design-software.html

Keywords: semi-continuous steel beam-to-column joints; global analysis; approximate determination of the joint stiffness; economical design; slim-floor construction

Authors:
Matthias Braun
ArcelorMittal Europe – Long Products
66, rue de Luxembourg
L-4009 Esch-sur-Alzette, Luxembourg

Job Duarte da Costa
Renata Obiala
Christoph Odenbreit
University of Luxembourg, FSTC
ArcelorMittal Chair of Steel & Façade Engineering
6, rue de Richard Coudenhove Kalergi
L-1359 Luxembourg, Luxembourg